MEARA Sequence Repeat of Human CstF-64 Polyadenylation Factor Is Helical in Solution. A Spectroscopic and Calorimetric Study†

John M. Richardson,‡,§ K. Wyatt McMahon,|| Clinton C. MacDonald,|| and George I. Makhatadze*,‡,§

Department of Chemistry & Biochemistry, Texas Tech University, Lubbock, Texas 79409, and Department of Cell Biology and Biochemistry, Texas Tech Health Sciences Center, Lubbock, Texas 79430

Received March 29, 1999; Revised Manuscript Received July 14, 1999

ABSTRACT: The primary structure of the human CstF-64 polyadenylation factor contains 12 nearly identical repeats of a consensus motif of five amino acid residues with the sequence MEAR(A/G). No known function has yet been ascribed to this motif; however, according to secondary structure prediction algorithms, it should form a helical structure in solution. To validate this theoretical prediction, we synthesized a 31 amino acid residue peptide ($MEARA_6$) containing six repeats of the MEARA sequence and characterized its structure and stability by circular dichroism (CD) spectroscopy and differential scanning calorimetry (DSC). No effects of concentration on the CD or DSC properties of $MEARA_6$ were observed, indicating that the peptide is monomeric in solution at concentrations up to 2 mM. The far UV−CD spectra of $MEARA_6$ indicates that at a low temperature (1 °C) the $MEARA_6$ peptide has a relatively high helical content (76% at pH 2.0 and 65% at pH 7.0). The effects of pH and ionic strength on the CD spectrum of $MEARA_6$ suggest that a number of electrostatic interactions (e.g., *i*, *i* + *3* Arg/Glu ion pair, charge−dipole interactions) contribute to the stability of the helical structure in this peptide. DSC profiles show that the melting of $MEARA_6$ helix is accompanied by positive change in the enthalpy. To determine thermodynamic parameters of helix−coil transition from DSC profiles for this peptide, we developed a new, semiempirical procedure based on the calculated function for the heat capacity of the coiled state for a broad temperature range. The application of this approach to the partial molar heat capacity function for $MEARA_6$ provides the enthalpy change for helix formation calculated per amino acid residue as 3.5 kJ/mol.

Mammalian cleavage stimulation factor (CstF)[1] is an essential factor for 3′-end processing and polyadenylation of pre-mRNA. The factor consists of three subunits with apparent molecular masses of 77, 64, and 50 kDa (*1*). The 64 kDa subunit (CstF-64) interacts directly with pre-mRNA downstream of the site of cleavage (*2*) in a polyadenylation signal- (AAUAAA-) dependent fashion (*3*). The primary structure of CstF-64 consists of 577 amino acid residues and can be conditionally divided into several domains (*4*). The N-terminal RNA-binding domain contains two ribonucleoprotein (RNP) motifs. Two Gly/Pro-rich domains for which no function has been described span residues 198−409 and 470−577. However, the most unusual feature seems to be a 60 amino acid domain (residues 409−469) with 12 repeats of the sequence MEAR(A/G) (Figure 1A). This feature is conserved in mouse (B. Dass and C.C.M. unpublished observations) and avian (*5*) versions of CstF-64, suggesting it has a significant biological function.

A

409 .IDARGMEARAMEARGLDARGLEARAMEARAMEARAMEARAMEARAMEVRGMEARGMDTRG. 469

B

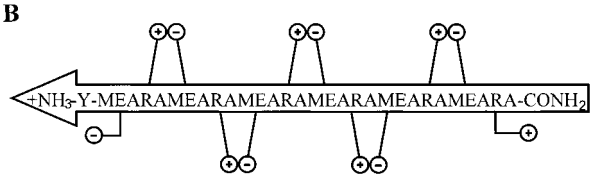

FIGURE 1: (A) Amino acid sequence of MEAR(A/G) domain of CstF-64 spanning residues 409−469 (*4*). Every second pentad of amino acid residues is underlined to accentuate the repetitiveness of the sequence. (B) Amino acid sequence of the $MEARA_6$ peptide and the cartoon representation of the peptide macrodipole (large arrow) and side-chain−side-chain interactions between arginine and glutamate residues.

Secondary structure algorithms predict a long α-helix (*4*) is formed by this domain. The alanine- and glycine-containing repeats are each present six times at the fifth position of MEAR(A/G) in the naturally occurring CstF-64 sequence. However the alanine-containing repeats are found

† This work was supported in part by grant from the NIH (GM54537 to G.I.M.), Robert A. Welch Foundation (D1403 to G.I.M.) and a grant from the Texas Tech University Health Sciences Center to C.C.M. Support for J.M.R. and K.W.M. was provided in part by a grant from the Howard Hughes Medical Institute through the Undergraduate Biological Sciences Education Program.

* Corresponding author.

‡ Present address: Department of Biochemistry and Molecular Biology, Penn State College of Medicine, Hershey, PA 17033. Phone (717) 531-0712; Fax (717) 531-7072; E-mail MAKHATADZE@PSU.EDU.

§ Texas Tech University.

|| Texas Tech Health Sciences Center.

[1] Abbreviations: CstF-64, 64 kDa subunit of the mammalian cleavage stimulation factor; $MEARA_6$, model peptide with the sequence NH_2-Y-$(MEARA)_6$-$CONH_2$; CD, circular dichroism; DSC, differential scanning calorimetry; TFE, 2,2,2-trifluoroethanol.

10.1021/bi990724r CCC: $18.00
Published on Web 09/11/1999

in the middle and the glycine-containing consensus repeats at the boundaries adjacent to the Gly/Pro-rich regions of CstF-64. Such sequence peculiarity raises the question of whether all the 60 amino acid residues in the MEAR(A/G) repeat indeed form a helical structure, since it is known that Gly is strongly disfavored in α-helical structures (*6*−*11*). In an attempt to shed more light on the possible structure of the MEAR(A/G) domain, we synthesized a 31 amino acid long peptide, $MEARA_6$, containing six repetitive MEARA sequences with one tyrosine residue to measure peptide concentrations. This synthetic peptide is expected to have a high degree of helicity since it is well-known that Ala-rich peptides form helical structures in solution (*12*−*15*). The presence of the straight side-chain amino acids Met and Arg, and γ-branched Glu in the Ala-rich sequence context also favors helix formation (*6*, *8*, *9*, *12*, *13*, *15*−*17*). The *i*, *i* + *3* spacing of arginine and glutamate promotes Arg/Glu ion pair formation (*18*−*23*). Finally, charge−helix macrodipole interactions between the first Glu residue and the N-terminus, and between the last Arg residue and the C-terminus, could also contribute to helix stability (Figure 1B).

Our study of the synthetic $MEARA_6$ peptide was designed to answer two major questions. First, is $MEARA_6$ peptide able to form a helical structure in solution? Second, does $MEARA_6$ exist as a monomer in solution or does it form oligomeric structures? Answers to each of these questions will have important implications for possible structures of CstF-64. If the $MEARA_6$ peptide is helical is solution, it increases the likelihood that this sequence will form a helical domain when it is part of the intact CstF-64 structure. Similarly, oligomerization of the $MEARA_6$ peptide in solution would suggest a role for this motif in dimerization or protein−protein interaction when it is part of the CstF-64 sequence. Using circular dichroism spectroscopy, we found that indeed the $MEARA_6$ peptide forms monomeric highly helical (65−76% depending on pH) structures in the solution. This finding suggests that the MEARA sequence repeat might form a helical structure when it is a part of the CstF-64 sequence but diminishes the possibility that it is involved in CstF-64 oligomerization.

After establishing that the MEARA sequence possess high helical content, we used differential scanning calorimetry (DSC) to measure directly the thermodynamics of helix−coil transition in this peptide. Analysis of the DSC data for helix−coil transition requires knowledge of the temperature dependence of the partial heat capacity of fully helical and fully coiled states of the peptide, information not accessible experimentally (*24*). To overcome this problem, we developed a new, semiempirical procedure based on the calculated function for the heat capacity of the coiled state for a broad temperature range.

MATERIALS AND METHODS

The $MEARA_6$ 31-residue peptide [actual sequence NH_2-Y-$(MEARA)_6$-$CONH_2$] was synthesized by solid-phase procedures on an automated peptide synthesizer (PE-Biosystems, Framingham, MA) using Fmoc protocols on a solid support resin (Fmoc-PAL-PEG-PS). At the end of synthesis, the peptide was cleaved from supporting resin by the standard TFA cleavage procedure (reagent R) followed by multiple ether extraction. The crude, lyophilized peptide was subjected to gel-filtration chromatography on Sephadex G-25 column to remove likely contaminants such as salts, scavengers, and small molecules. The elution position of the peptide was identified by RP-HPLC (Waters, Milford, MA) on a C4 analytical column followed by ESI-mass spectrometry with a triple-quadrupole instrument (VG Quattro II, Fisons Instruments). The peptide was purified on a RP-HPLC C4 semipreparative column with a gradient of 5−70% acetonitrile with 0.1% TFA. The identity of the $MEARA_6$ peptide was checked by ESI-mass spectrometry (determined molecular mass 3530.5 Da as compared to the expected value of 3533 Da). $MEARA_6$ in a given buffer solution was prepared by dialysis through SpectraPor membranes with a molecular weight cutoff of 1000. Prior to experiments the peptide solutions were clarified by centrifugation at 13000*g* for 20−25 min at 4 °C. The concentration of $MEARA_6$ in solution was measured spectrophotometrically with an extinction coefficient $E^{0.1\%}_{1cm,276nm}$ of 0.41, calculated by the method as described (*25*).

Circular dichroism (CD) measurements were made with a Jasco J-715 spectropolarimeter. Temperature was controlled by a Neslab automated circulating water bath. Spectra of peptide solutions were measured in a 1 cm water-jacketed cylindrical quartz cell for melting experiments or a 1 cm rectangular quartz cell for the NaCl and 2,2,2-trifluoroethanol (TFE) titrations. Measured spectra were corrected for buffer effects and normalized per peptide concentration, which was varied from 3 to 14 μM. Ellipticity is expressed per mole of amino acid residues with 114 Da as an average residue molecular mass. All CD experiments were performed in buffers containing 10 mM NaCl, and 1 mM each of sodium phosphate, sodium borate, sodium citrate (CD buffer) as described previously (*23*, *25*, *26*). TFE solutions were prepared using procedure described (*27*).

Fractional helicity of the $MEARA_6$ peptide, f_H, was determined from the mean residue ellipticity at 222 nm, $[\Theta]_{222}$, as

$$f_H = \frac{[\Theta]_{222} - [\Theta]_C}{[\Theta]_H - [\Theta]_C} \quad (1)$$

where $[\Theta]_C$ and $[\Theta]_H$ are the ellipticities of the fully coiled and fully helical states, respectively. The ellipticity of the fully coiled state depends on the temperature, *T* (in degrees Celsius), as (*15*)

$$[\Theta]_C = 640 - 45T \quad (2)$$

The ellipticity of the fully helical peptide, $[\Theta]_H$, with the number of residues in the peptide, N_r, is related to the ellipticity of the complete helix of infinite length, $[\Theta]^\infty_H$, as

$$[\Theta]_H = [\Theta]^\infty_H\{1 - (2.5/N_r)\} \quad (3)$$

where the $[\Theta]^\infty_H$ dependence on temperature (in degrees Celsius) was suggested to be a linear function (*15*):

$$[\Theta]^\infty_H = -40\,000 + \frac{\partial[\Theta]^\infty_H}{\partial T}T \quad (4)$$

Two different values for the temperature dependence, $\partial[\Theta]^\infty_H/\partial T$, have been reported (*28*, *29*): 125 or 250 de-

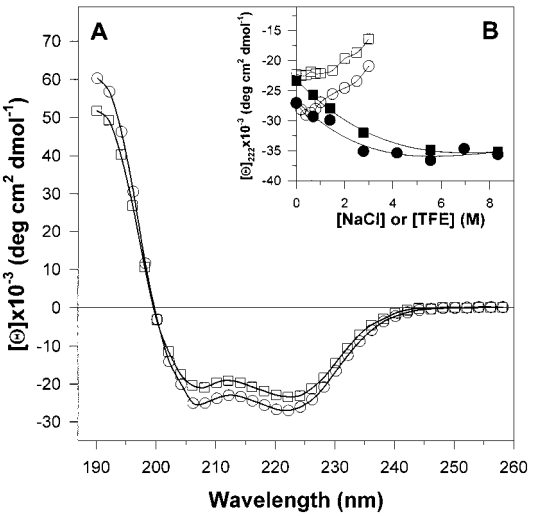

FIGURE 2: (A) Circular dichroism spectra of $MEARA_6$ at 1 °C at pH 2.0 (○) or pH 7.0 (□). Each spectrum is an average of at least five independent measurements. The standard deviations of the measurements are approximately of the size of the symbols. (B) Ellipticity of $MEARA_6$ peptide as a function of NaCl (open symbols) or TFE (solid symbols) concentration at 1 °C at pH 2.0 (○, ●) or pH 7.0 (□, ■).

pending on the method of estimation (*15*). For a detailed discussion of the temperature dependence of the ellipticity for fully helical reference state for $MEARA_6$ see Results and Discussions.

Differential scanning calorimetry (DSC) experiments were performed with a VP-DSC (Microcal Inc.) instrument (*30*) at $MEARA_6$ concentrations from 1 to 5 mg/mL as described elsewhere (*31*). The partial molar heat capacity of $MEARA_6$ in solution was calculated with a partial molar volume of 0.721 cm^3/g (*32*). Scan rates in each experiment was 90 deg/h. Reversibility of transition was checked by reheating the same sample.

RESULTS AND DISCUSSION

Structural Characterization of $MEARA_6$ in Solution by CD Spectroscopy. Figure 2A compares the spectra of $MEARA_6$ peptide at 1 °C at pH 2.0 and 7.0. Under both conditions the spectrum is consistent with α-helical structure, characterized by well-pronounced minima at 222 and 207 nm and positive ellipticity at 190 nm. The absolute values of ellipticity are larger at pH 2.0 ($[\Theta]_{222} = -27\,000$ deg·cm^2·dmol^{-1}) than at pH 7.0 ($[\Theta]_{222} = -23\,400$ deg·cm^2·dmol^{-1}), indicating a somewhat higher helical content at the lower pH. Spectra of $MEARA_6$ were obtained at several concentrations of peptide differing by factors of 12, 25, 37, and 50. Spectra at all concentrations were practically superimposable, indicating that the peptide is monomeric in solution at both neutral and acid pH (data not shown). The effect of pH on the ellipticity of $MEARA_6$ is qualitatively in good agreement with earlier results obtained on several different peptide design incorporating Arg/Glu (*33*), or Lys/Glu (*21*, *34*, *35*) pairs in *i*, *i* + *3* spacing. In each peptide ellipticity at 222 nm was more negative at low pH than at pH 7.0, which agrees with our data for $MEARA_6$.

The difference in ellipticity of $MEARA_6$ at pH 2.0 and 7.0 can be attributed to at least four different factors, contributing simultaneously to the stability of the peptide. First is the effect of titration of glutamate on the intrinsic helix propensity of this residue. It is known that neutral glutamate, Glu^0, which is present in $MEARA_6$ at pH 2.0, has much higher intrinsic helical propensity than the charged glutamate, Glu^-, present at pH 7.0 (*13*, *35*, *36*). Second is the effect of electrostatic interactions at the helix end (*12*, *13*, *15*, *36*). At pH 7.0, favorable interactions are present on both ends of the $MEARA_6$ peptide: side chain of Glu^- with the N-terminus and side chain of Arg^+ with the C-terminus (Figure 1). At pH 2.0, due to the protonation of the glutamate, the stabilizing interaction at the N-terminus vanishes. Third, the strength of the Arg−Glu ion pair will decrease upon pH decrease from 7.0 to 2.0. Smith and Scholtz (*23*) showed that the protonation of the acidic residue in an ion pair leads to a decrease in helix stability. This decrease, however, is not very large. For example, in the analysis of Smith and Scholtz the energy of interactions of the Lys^+-Glu^- ion pair was estimated to be 280 cal/mol compared to 235 cal/mol for the Lys^+-Glu^0 pair. Fourth, a change in pH has an effect on charged side chain−helix macrodipole interactions. These interactions are overall unfavorable for the Arg/Glu-type orientation as opposed to the Glu/Arg-type orientation. This effect of relative orientation of ion pair relative to the helix macrodipole influences not only the absolute value of ellipticity but also the effect of pH on $[\Theta]_{222}$ (*15*, *21*, *23*, *33*, *34*). Protonation of one of the partners in the Arg/Glu ion pair upon pH decrease from 7.0 to 2.0 will lead to a decrease in the unfavorable charge−helix dipole interactions, thus increasing the overall helix stability. An attempt to quantify the charge−helix dipole interactions was undertaken by Huyghues-Despointes et al. (*33*), using the effect of ionic strength on the ellipticity of model peptides. They observed effects qualitatively similar to the effects of NaCl concentrations on ellipticity of $MEARA_6$, i.e., an increase in $[\Theta]_{222}$ at NaCl concentrations above 1 M (Figure 2B). Exact enumeration of different electrostatic contributions to the stability of this peptide will require further study by the approaches developed by Smith and Scholtz (*23*) and Huyghues-Despointes et al. (*33*).

Prior to converting $[\Theta]_{222}$ values into mean helical fraction, we established an experimental baseline for the 100% helical structure. This was done by adding 2,2,2-trifluoroethanol (TFE) to $MEARA_6$ in solution. TFE was chosen because high concentrations of TFE are known to increase the helical content of peptides with significant helical structure in water to almost 100% (*29*). Figure 2B shows the effect of the increasing concentrations of TFE on the $[\Theta]_{222}$ values of $MEARA_6$ at pH 2.0 and 7.0 at 1 °C. The values of $[\Theta]_{222}$ become more negative with the increase in concentration of TFE, approaching a plateau at $-35\,500$ deg·cm^2·dmol^{-1}. This plateau value was independent of the pH (2.0 or 7.0) but was reached at a different concentration of TFE at each pH. At pH 2.0 the plateau value was reached at ∼3 M (20% v/v) TFE, whereas at pH 7.0 the same ellipticity is reached at ∼5 M (35% v/v) TFE. This difference in the concentration of TFE required to reach the saturation of $[\Theta]_{222}$ might be a consequence of the difference in $[\Theta]_{222}$ for no TFE at these pH values. A similar plateau value at different pH might serve as an indication that at high concentrations of TFE, $MEARA_6$ has similar and presumably 100% helical content at 1 °C. Additional support for this conclusion comes from the estimates of $[\Theta]_{222}$ from eq 3 for a fully helical 31-mer peptide. Equation 3 calculates that the $MEARA_6$ peptide in

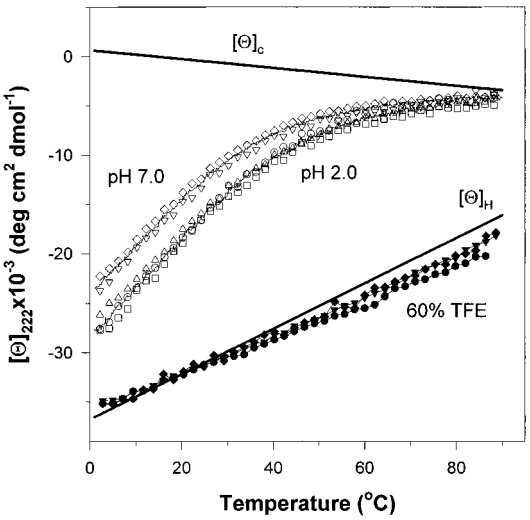

FIGURE 3: Temperature dependence of $[\Theta]_{222}$ of the $MEARA_6$ peptide. The profiles were obtained at pH 2.0 (○, □, △) and pH 7.0 (◇, ▽) or in 60% TFE at pH 2.0 (●) and pH 7.0 (◆, ▼). The concentrations of $MEARA_6$ for each experiment were 14 μM (○, ◇), 35 μM (□), 90 μM (△, ▽), 8 μM (●, ◆), and 3 μM (▼). The thick solid lines show the temperature dependence of the ellipticity at 222 nm for the random coil ($[\Theta]_C$, eq 2) or completely helical peptide 31 amino acids long ($[\Theta]_H$, eq 4).

a fully helical conformation at 1 °C will have an ellipticity of $-36\,500$ deg·cm^2·dmol^{-1}. This value is in close agreement with the observed plateau value of $-35\,500$ deg·cm^2·dmol^{-1} for ellipticity at 222 nm that was measured experimentally from the TFE titration (Figures 2B and 3), suggesting that at high concentrations of TFE at 1 °C, $MEARA_6$ was nearly 100% helical. Knowing the expected values of $[\Theta]_{222}$ for the coil (eq 2) and for the fully helical peptide (eq 3), we were able to estimate the fraction of $MEARA_6$ peptide in the helical conformation by using eq 1. It was found that in the absence of TFE at 1 °C the fraction of $MEARA_6$ residues in helical conformation is 76% ± 3% and 65% ± 3% at pH 2.0 and 7.0, respectively.

Figure 3 shows changes in $[\Theta]_{222}$ values of $MEARA_6$ as a function of temperature. The melting profiles of $MEARA_6$ obtained at different peptide concentrations and different pH values overlap, indicating that $MEARA_6$ is monomeric in solution at both low and high temperatures and over a range of pH values. As expected, the absolute value of ellipticity of $MEARA_6$ at 222 nm decreases with the increase in temperature and reaches an apparent saturation at ~90 °C. The $[\Theta]_{222}$ values for $MEARA_6$ at pH 2.0 and 7.0 approach, at high temperatures, the ellipticity values calculated for the fully coiled peptide according to eq 2, suggesting that the peptide is fully unfolded at high temperatures (Figure 3).

To calculate the temperature dependence of the fraction of $MEARA_6$ in helical conformation we used eq 1, with the temperature dependencies of the ellipticities for the coiled, $[\Theta]_C$, and fully helical, $[\Theta]_H$, states defined by eqs 2 and 3, respectively. Although the temperature dependence of ellipticity for the coiled state is well-defined (*15*), the temperature dependence of ellipticity of fully helical peptide is not. Two different values for the temperature dependence of ellipticity $\partial[\Theta]_H^\infty/\partial T$ have been reported (*28*, *29*): 125 and 250 deg·cm^2·dmol^{-1}·°C^{-1}. The expected ellipticity for fully helical $MEARA_6$ peptide at low temperature is in excellent correspondence with the experimental ellipticity

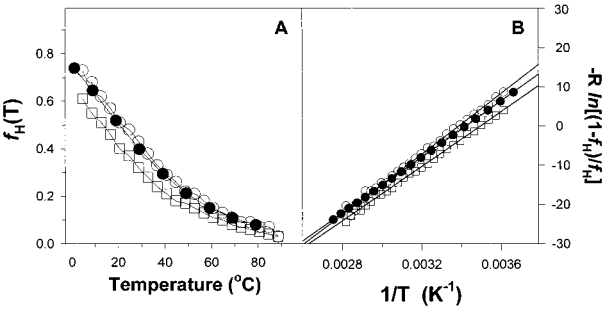

FIGURE 4: (A) Temperature dependence of the mean helix content, $f_H(T)$, at pH 2.0 (○) or pH 7.0 (□) calculated from the CD data using eq 1 or at pH 2.0 (●) from the analysis of DSC data shown in Figure 5. Continuous lines drawn through the points do not carry any meaning but are only meant to guide the eye. (B) van't Hoff plot for $MEARA_6$ unfolding monitored by CD at pH 2.0 (○) and pH 7.0 (□) or by DSC at pH 2.0 (●). The fits of the individual data to the van't Hoff equation gave the following estimates for the enthalpy and entropy changes: 36 kJ/mol and -122 J/(K·mol) for DSC; 38 kJ/mol and -129 J/(K·mol) for CD at pH 2.0; and 35 kJ/mol and -123 J/(K·mol) for CD at pH 7.0.

of $MEARA_6$ in high concentrations of TFE, in which the helix-forming peptides are usually assumed to have close to 100% helical content (*29*). The temperature dependence of $MEARA_6$ in 9 M (60%) TFE estimated from the linear fit of the experimental data (Figure 3) obtained at different pH values and peptide concentrations is 190 deg·cm^2·dmol^{-1}·°C^{-1}. This value for $MEARA_6$ translates into 210 deg·cm^2·dmol^{-1}·°C^{-1} for the infinite helix, very close to the estimate of 250 deg·cm^2·dmol^{-1}·°C^{-1} by Baldwin and co-workers (*15*, *29*). Our experimental estimate of 190 deg·cm^2·dmol^{-1}·°C^{-1}, however, implies that in 9 M (60%) TFE the amount of helical structure in $MEARA_6$ peptide is independent of temperature.

Using the value of 250 deg·cm^2·dmol^{-1}·°C^{-1} for the temperature dependence of the ellipticity of an infinite helix, the fraction of helical structure, f_H, in $MEARA_6$ at the two different pH values will have dependencies as shown in Figure 4A. The temperature dependence of f_H allows us to calculate the van't Hoff enthalpy, ΔH_{vH}, from the slope of the dependence of $-R \ln[(1 - f_H)/f_H]$ on $1/T$ (Figure 4B). This analysis gives estimates for ΔH_{vH} of 38 and 35 kJ/mol at pH 2.0 and 7.0, respectively. These estimates can be compared with the results obtained on a 51 residue peptide analyzed by Scholtz et al. (*24*). They determined a value for ΔH_{vH} of 47 kJ/mol at pH 7.0, or 0.94 kJ/mol per amino acid residue. This compares to the value of 1.1 kJ/mol per amino acid residue for $MEARA_6$. The correspondence between two sets of data is remarkable, keeping in mind the wealth of knowledge, both experimental and theoretical, on helix stability accumulated in the past decade (*15*, *37*, *38*). The van't Hoff enthalpy, however, represents an enthalpy of a two-state state transition of 1 mol of cooperative unit, which in the case of helix-coil transition is not the same as 1 mol of peptide (*23*, *24*, *28*, *29*, *39*). To determine the true enthalpy associated with the helix−coil transition, we used the more direct method of differential scanning calorimetry, DSC (*31*, *40*).

Thermodynamics of $MEARA_6$ Unfolding from DSC. The DSC profiles for $MEARA_6$ peptide at pH 2.0 are shown in Figure 5. Complexity of analysis of the DSC data depends on two parameters: reversibility of the observed reaction

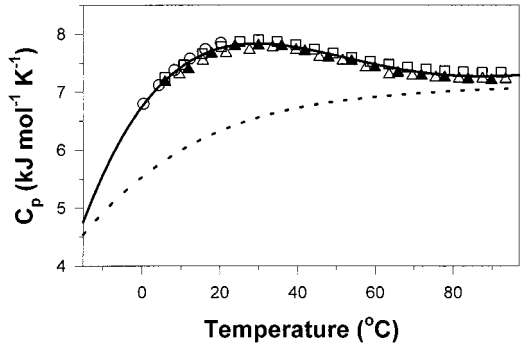

FIGURE 5: Temperature dependence of the partial molar heat capacity of $MEARA_6$ in 20 mM glycine hydrochloride buffer, pH 2.0. The DSC profiles were obtained at the concentrations of peptide of 1.6 mM (○, □) or 0.4 mM (△, ▲) by scanning the samples up (□, △), down (○), or rescanning (▲). The thick solid line represents the expected DSC profile for the helix−coil transition calculated with the $\Delta H = 107$ kJ/mol. The dotted line represents the partial molar heat capacity of $MEARA_6$ in the unfolded conformation, $C_{p,U}(T)$, calculated by using the additivity scheme (*31*, *51*).

and molecularity of this reaction (*31*). The helix−coil transition of $MEARA_6$ at pH 2.0 seems to be a monomolecular reaction. The DSC profiles obtained at two different concentrations of $MEARA_6$ (0.4 and 1.6 mM) are superimposable. This points out that even at these higher concentrations (as compared to CD experiments), $MEARA_6$ exists in a monomeric state over a temperature range from 0 to 95 °C. The heat-induced helix−coil transition in $MEARA_6$ peptide was also fully reversible, as was seen from the high reproducibility of the calorimetric profiles obtained upon two consequent heatings of the same sample (Figure 5).

Although the heat-induced transition reaction of $MEARA_6$ is reversible and monomolecular, analysis of the DSC profile presents a challenge because helix−coil transition in isolated helical peptides cannot be described by a simple two-state transition model (*12*, *23*, *24*, *28*, *29*, *39*, *41*, *42*). Following the classical work of Biltonen and Freire (*43*), the first step in the analysis of DSC profiles is the determination of the excess heat capacity function $\langle C_p(T)\rangle^{exc}$, the heat capacity caused exclusively by the heat released or absorbed during the reaction. The importance of the $\langle C_p(T)\rangle^{exc}$ function follows from the fact that the area under it represents the enthalpy of the reaction in study, i.e.

$$\Delta H_{cal} = \int_{T_1}^{T_2} \langle C_p(T)\rangle^{exc}\, dT \qquad (5)$$

The excess heat capacity function $\langle C_p(T)\rangle^{exc}$ is expressed as a difference between the experimental, $C_p^{exp}(T)$, and progress, $C_p^{prg}(T)$, heat capacity functions (*31*):

$$\langle C_p(T)\rangle^{exc} = C_p^{exp}(T) - C_p^{prg}(T) \qquad (6)$$

The progress heat capacity is defined by intrinsic (partial) heat capacity over the entire temperature range:

$$C_p^{prg}(T) = F_N(T)C_{p,N}(T) + F_U(T)C_{p,U}(T) \qquad (7)$$

where $C_{p,N}(T)$ and $C_{p,U}(T)$ are the temperature dependencies of the partial heat capacities of the initial (native) and final (unfolded) states, respectively, and $F_N(T)$ and $F_U(T)$ are the fractions of the protein in the initial (native) and final (unfolded) states.

In the case of highly cooperative two-state transitions, such as those observed for globular proteins (*31*, *40*), the heat capacities of the initial (native) and final (unfolded) states are well-defined, can be measured experimentally, and can be used to determine the excess heat capacity function (*31*, *43*). In the case of the helix−coil transition the heat capacity function of the initial fully helical state is not accessible experimentally and only the final unfolded state can be defined relatively well. Thus, to determine the excess heat capacity function, one needs to define the progress heat capacity function by an empirical approach. There are several ways of defining the progress heat capacity function for helix−coil transitions (*24*). Each is based on a fitting procedure that divides a helix−coil transition into a large number of two-state transitions determined by the temperature-independent enthalpy. While such a procedure might not be strictly valid for a helix−coil transition, it appears to yield values similar to our estimates of the enthalpy of helix melting.

We developed a new procedure for the determination of the enthalpy of the helix−coil transition from calorimetric data. This procedure is based on two premises. First, the heat capacity change upon helix−coil transition, $\Delta C_p = C_{p,U} - C_{p,N}$, is very small and can be assumed in a first approximation to be zero, i.e., $C_{p,N} = C_{p,U}$. Indeed, according to the currently accepted view, the heat capacity change upon unfolding is caused mainly by the hydration of the newly exposed surface areas of the group buried in the initial state, with polar and nonpolar groups having contributions of opposite signs (e.g., refs *44*−*47*). Theoretical calculations suggest that the amount of surface area exposed upon helix unfolding is small and involves both polar and nonpolar groups (*48*−*50*). Second, at high temperatures a peptide exists in the unfolded state, as follows from the close correspondence of the $[\Theta]_{222}$ values for $MEARA_6$ obtained at high temperatures and ellipticity values for the coiled state, calculated according to eq 2 (Figure 3). On the basis of these two premises, eq 7 can rewritten as

$$C_p^{prg}(T) = [F_N(T) + F_U(T)]C_{p,U}(T) = C_{p,U}(T) \qquad (8)$$

Thus the knowledge of the heat capacity function for the unfolded peptide will allow the estimation of the progress heat capacity function and thus of the excess heat capacity function, which carries the information about the enthalpy of the process.

Several years ago, Makhatadze and Privalov (*44*, *45*, *51*) developed a semiempirical approach for predicting the partial molar heat capacity functions of proteins and peptides in the unfolded state. This approach requires the knowledge of the amino acid composition of the given polypeptide and allows calculations of the partial molar heat capacity as

$$C_{p,U}^{calc}(T) = \sum_i n_i \hat{C}_{p,i}(T) + (N-1)C_{p,CHCONH}(T) \qquad (9)$$

where N is the total number of amino acid residues in the sequence, n_i is the number of ith type amino acid residue, $\hat{C}_{p,i}(T)$ is the partial molar heat capacity for the side chain of the ith type, and $C_{p,CHCONH}(T)$ is the partial molar heat capacity for the peptide unit. The values of $\hat{C}_{p,i}(T)$ and $C_{p,CHCONH}(T)$ have been derived for all 20 amino acid residues

and for the peptide unit from the experimentally measured partial molar heat capacities of model compounds for the temperature range from 5 to 125 °C (*44*). It has been shown that the calculated (eq 9) and experimentally measured heat capacity functions for the unfolded states of more than a dozen of proteins and peptides coincide with very good accuracy (*45*, *52*). The same is observed for the $MEARA_6$ peptide, where the calculated and experimental values for the partial molar heat capacity are very close at high temperatures (Figure 5). This indicates that indeed the state of the $MEARA_6$ peptide at high temperatures is very close to the unfolded coiled state, in agreement with the results of the CD experiments (see Figure 3). Similarity between the calculated and experimentally measured heat capacities of $MEARA_6$ at high temperatures also indicates that we can use the function calculated according to eq 9 to define the expected heat capacity function of the unfolded $MEARA_6$. Thus, we can define the progress heat capacity (eqs 7 and 8) and ultimately, the excess heat capacity function for $MEARA_6$ (Figure 5).

The integral of the experimental and the progress heat capacity functions from 0 to 95 °C (Figure 5) represents the heat of helix−coil transition estimated at 80 kJ/mol. Since we have shown from the analysis of CD spectra at pH 2.0 and 0 °C that $MEARA_6$ is ∼75% helical, the enthalpy of 100% helix to coil transition in $MEARA_6$ peptide will be 107 kJ/mol, or 3.5 kJ/mol of amino acid residues. This enthalpy is in excellent correspondence with the enthalpy of 3.8 kJ/mol of residues obtained by Scholtz et al. (*24*) on the 51 residue Ala-based peptide using a simpler "baseline flooring" procedure for analysis of the DSC data. The enthalpy of helix−coil transition of ∼3.5 kJ/mol supports previous theoretical and empirical estimates that helix formation is accompanied by relatively low enthalpy values (*15*, *29*, *45*, *46*, *50*, *53*). Knowing the enthalpy of helix−coil transition, one can calculate the heat capacity profile for the $MEARA_6$ peptide at pH 2.0 even for temperatures below the freezing point of water (Figure 5). It appears that 100% helical structure will be populated around −25 °C, outside experimentally accessible temperature range. It also allows us to estimate the van't Hoff enthalpy of unfolding, ΔH_{vH}, from the slope of the $-R \ln [(1 - f_H)/f_H]$ vs $1/T$ function (Figure 4B). This analysis shows that the van't Hoff enthalpy (36 kJ/mol) is lower than the calorimetric enthalpy (107 kJ/mol) by a factor of ∼3, thus providing additional evidence for the non-two-state character of the transition in $MEARA_6$. The van't Hoff enthalpy obtained from the $[\Theta]_{222}$ melting profiles (Figure 4) is 38 kJ/mol, in excellent agreement with the ΔH_{vH} obtained from the DSC data. The mean helical fractions, $f_H(T)$, obtained from the CD and DSC experiments change in a similar way (Figure 4A), indicating that both spectroscopic and calorimetric methods, and the corresponding analysis, describe the same process, i.e., helix to coil transition in the $MEARA_6$ peptide.

The stability of a helical peptide in aqueous solution is defined not only by the enthalpic factors but also by the entropic factors. Indirect evidence for this assertion follows from the van't Hoff analysis of the thermally induced transition of $MEARA_6$. The $-R \ln [(1 - f_H)/f_H]$ vs $1/T$ plot gives the estimate for the entropy, ΔS, of $MEARA_6$ melting of −125 J/(K·mol). This provides an indication that the helical structure of $MEARA_6$ is stabilized not only by enthalpic, ΔH, but also by entropic, $-T\Delta S$, contributions. This conclusion is in accord with earlier semiempirical estimates of noncovalent factors important for protein stability (*45*) and with theoretical predictions (*53*). These studies argued that dehydration of the peptide backbone upon helix formation had an important contribution to helix stability, a contribution that was qualitatively similar to the effect observed on the $MEARA_6$ peptide.

CONCLUDING REMARKS

Far-UV CD spectroscopy of the synthetic $MEARA_6$ peptide shows that it is monomeric and that the $MEARA_6$ sequence can adopt a highly (>65%) helical conformation in aqueous solution. This suggests that the MEARA sequence as a part of the intact CstF-64 molecule might also adopt an α-helical conformation (*36*, *54*−*57*). We must note, however, that there are reported instances where a given sequence can adopt two different conformations depending on the context with which it is inserted (*58*) or where the structure of the peptide in solution is different from the structure in the intact protein (*59*). The Paracelcius challenge (*60*, *61*), and successful (*62*) and not so successful (*63*, *64*) attempts to meet this challenge also alerts us to the possibility that tertiary interactions can be more important in defining the final "look" of the folded protein structure. While $MEARA_6$ is almost certainly helical under all conditions of physiological interest, we cannot say with the same certainty that this is true of MEAR(A/G) repeat seen in the CstF-64 protein. In particular, the glycine residues in the fifth position in six out of the 12 repeats would tend to destabilize the helix. Additionally, the structural contributions of the Gly/Pro-rich domains that flank the MEAR(A/G) repeat are not yet clear. Further experiments will be required to address these issues.

As a model peptide, $MEARA_6$ seems to be a useful tool to evaluate the contributions of different forces to the helix stability. Using more precise DSC instrumentation and a new approach to analyze the DSC profiles for helix−coil transition, we were able to estimate the enthalpy of helix−coil transition to be relatively small, on the order of 3.5 kJ/mol of amino acid residue. This enthalpy change is at least several times smaller than the enthalpy of unfolding of small globular proteins. The stability of an isolated helical peptide in solution is not defined solely by the enthalpic factor. It appears that the entropic factor, arising presumably from dehydration of the peptide backbone upon helix formation, can be a significant contributor to the helix stability.

ACKNOWLEDGMENT

We express our deep appreciation to Dr. Marty Scholtz (Texas A&M) for numerous discussions on the manuscript and invaluable suggestions. We also thank Kazi Islam for synthesis of the $MEARA_6$ peptide.

REFERENCES

1. Takagaki, Y., Manley, J. L., MacDonald, C. C., Wilusz, J., and Shenk, T. (1990) *Genes Dev. 4*, 2112−2120.
2. MacDonald, C. C., Wilusz, J., and Shenk, T. (1994) *Mol. Cell. Biol. 14*, 6647−6654.
3. Wilusz, J., and Shenk, T. (1988) *Cell 52*, 221−228.
4. Takagaki, Y., MacDonald, C. C., Shenk, T., and Manley, J. L. (1992) *Proc. Natl. Acad. Sci. U.S.A. 89*, 1403−1407.

5. Takagaki, Y., and Manley, J. L. (1998) *Mol. Cell 2*, 761−771.
6. O'Neil, K. T., and DeGrado, W. F. (1990) *Science 250*, 646−651.
7. Chakrabartty, A., Schellman, J. A., and Baldwin, R. L. (1991) *Nature 351*, 586−588.
8. Lyu, P. C., Liff, M. I., Marky, L. A., and Kallenbach, N. R. (1990) *Science 250*, 669−673.
9. Creamer, T. P., and Rose, G. D. (1992) *Proc. Natl. Acad. Sci. U.S.A. 89*, 5937−5941.
10. Serrano, L., Neira, J. L., Sancho, J., and Fersht, A. R. (1992) *Nature 356*, 453−455.
11. Blaber, M., Zhang, X. J., Lindstrom, J. D., Pepiot, S. D., Baase, W. A., and Matthews, B. W. (1994) *J. Mol. Biol. 235*, 600−624.
12. Scholtz, J. M., and Baldwin, R. L. (1992) *Annu. Rev. Biophys. Biomol. Struct. 21*, 95−118.
13. Chakrabartty, A., and Baldwin, R. L. (1995) *Adv. Protein Chem. 46*, 141−176.
14. Huyghues-Despointes, B. M., Scholtz, J. M., and Baldwin, R. L. (1993) *Protein Sci. 2*, 1604−1611.
15. Rohl, C. A., and Baldwin, R. L. (1998) *Methods Enzymol. 295*, 1−26.
16. Creamer, T. P., and Rose, G. D. (1994) *Proteins: Struct., Funct., Genet. 19*, 85−97.
17. Yang, J., Spek, E. J., Gong, Y., Zhou, H., and Kallenbach, N. R. (1997) *Protein Sci. 6*, 1264−1272.
18. Stellwagen, E., Park, S. H., Shalongo, W., and Jain, A. (1992) *Biopolymers 32*, 1193−1200.
19. Lyu, P. C., Gans, P. J., and Kallenbach, N. R. (1992) *J. Mol. Biol. 223*, 343−350.
20. Park, S. H., Shalongo, W., and Stellwagen, E. (1993) *Biochemistry 32*, 12901−12905.
21. Marqusee, S., and Baldwin, R. L. (1987) *Proc. Natl. Acad. Sci. U.S.A. 84*, 8898−8902.
22. Munoz, V., and Serrano, L. (1995) *Curr. Opin. Biotechnol. 6*, 382−386.
23. Smith, J. S., and Scholtz, J. M. (1998) *Biochemistry 37*, 33−40.
24. Scholtz, J. M., Marqusee, S., Baldwin, R. L., York, E. J., Stewart, J. M., Santoro, M., and Bolen, D. W. (1991) *Proc. Natl. Acad. Sci. U.S.A. 88*, 2854−2858.
25. Pace, C. N., Vajdos, F., Fee, L., Grimsley, G., and Gray, T. (1995) *Protein Sci. 4*, 2411−2423.
26. Smith, J. S., and Scholtz, J. M. (1996) *Biochemistry 35*, 7292−7297.
27. Nelson, J. W., and Kallenbach, N. R. (1986) *Proteins: Struct., Funct., Genet. 1*, 211−217.
28. Scholtz, J. M., Qian, H., York, E. J., Stewart, J. M., and Baldwin, R. L. (1991) *Biopolymers 31*, 1463−1470.
29. Luo, P., and Baldwin, R. L. (1997) *Biochemistry 36*, 8413−8421.
30. Plotnikov, V. V., Brandts, J. M., Lin, L. N., and Brandts, J. F. (1997) *Anal. Biochem. 250*, 237−244.
31. Makhatadze, G. I. (1998) *Current Protocols in Protein Chemistry*, Vol. 2, John Wiley & Sons, New York.
32. Makhatadze, G. I., Medvedkin, V. N., and Privalov, P. L. (1990) *Biopolymers 30*, 1001−1010.
33. Huyghues-Despointes, B. M., Scholtz, J. M., and Baldwin, R. L. (1993) *Protein Sci. 2*, 80−85.
34. Marqusee, S., Robbins, V. H., and Baldwin, R. L. (1989) *Proc. Natl. Acad. Sci. U.S.A. 86*, 5286−5290.
35. Scholtz, J. M., Qian, H., Robbins, V. H., and Baldwin, R. L. (1993) *Biochemistry 32*, 9668−9676.
36. Pace, C. N., and Scholtz, J. M. (1998) *Biophys. J. 75*, 422−427.
37. Kallenbach, N. R., and Spek, E. J. (1998) *Methods Enzymol. 295*, 26−41.
38. Aurora, R., Creamer, T. P., Srinivasan, R., and Rose, G. D. (1997) *J. Biol. Chem. 272*, 1413−1416.
39. Jasanoff, A., and Fersht, A. R. (1994) *Biochemistry 33*, 2129−2135.
40. Privalov, P. L. (1979) *Adv. Protein Chem. 33*, 167−241.
41. Merutka, G., Morikis, D., Bruschweiler, R., and Wright, P. E. (1993) *Biochemistry 32*, 13089−13097.
42. Wright, P. E., Dyson, H. J., and Lerner, R. A. (1988) *Biochemistry 27*, 7167−7175.
43. Biltonen, R. L., and Freire, E. (1978) *CRC Crit. Rev. Biochem. 5*, 85−124.
44. Makhatadze, G. I., and Privalov, P. L. (1990) *J. Mol. Biol. 213*, 375−384.
45. Makhatadze, G. I., and Privalov, P. L. (1995) *Adv. Protein Chem. 47*, 307−425.
46. Oobatake, M., and Ooi, T. (1993) *Prog. Biophys. Mol. Biol. 59*, 237−284.
47. Spolar, R. S., Livingstone, J. R., and Record, M. T., Jr. (1992) *Biochemistry 31*, 3947−3955.
48. Creamer, T. P., Srinivasan, R., and Rose, G. D. (1995) *Biochemistry 34*, 16245−16250.
49. Creamer, T. P., Srinivasan, R., and Rose, G. D. (1997) *Biochemistry 36*, 2832−2835.
50. Luque, I., Mayorga, O. L., and Freire, E. (1996) *Biochemistry 35*, 13681−13688.
51. Privalov, P. L., and Makhatadze, G. I. (1990) *J. Mol. Biol. 213*, 385−391.
52. Makhatadze, G. I. (1998) *Biophys. Chem. 71*, 133−156.
53. Yang, A. S., and Honig, B. (1995) *J. Mol. Biol. 252*, 351−365.
54. Myers, J. K., Smith, J. S., Pace, C. N., and Scholtz, J. M. (1996) *J. Mol. Biol. 263*, 390−395.
55. Myers, J. K., Pace, C. N., and Scholtz, J. M. (1997) *Biochemistry 36*, 10923−10929.
56. Myers, J. K., Pace, C. N., and Scholtz, J. M. (1997) *Proc. Natl. Acad. Sci. U.S.A. 94*, 2833−2837.
57. Myers, J. K., Pace, C. N., and Scholtz, J. M. (1998) *Protein Sci. 7*, 383−388.
58. Minor, D. L., Jr., and Kim, P. S. (1996) *Nature 380*, 730−734.
59. Hamada, D., Kuroda, Y., Tanaka, T., and Goto, Y. (1995) *J. Mol. Biol. 254*, 737−746.
60. Rose, G. D., and Creamer, T. P. (1994) *Proteins: Struct., Funct., Genet. 19*, 1−3.
61. Rose, G. D. (1997) *Nat. Struct. Biol. 4*, 512−514.
62. Dalal, S., Balasubramanian, S., and Regan, L. (1997) *Nat. Struct. Biol. 4*, 548−552.
63. Jones, D. T., Moody, C. M., Uppenbrink, J., Viles, J. H., Doyle, P. M., Harris, C. J., Pearl, L. H., Sadler, P. J., and Thornton, J. M. (1996) *Proteins: Struct., Funct., Genet. 24*, 502−513.
64. Yuan, S. M., and Clarke, N. D. (1998) *Proteins: Struct., Funct., Genet. 30*, 136−143.

BI990724R